Journal Name

RSCPublishing

Copper reduction and atomic layer deposition by oxidative decomposition of formate by hydrazine

Cite this: DOI: 10.1039/x0xx00000x

Gangotri Dey[a], and Simon D. Elliott[b]

Received 00th January 2012,
Accepted 00th January 2012

DOI: 10.1039/x0xx00000x

www.rsc.org/

WE HAVE USED DENSITY FUNCTIONAL THEORY (DFT) TO STUDY THE MECHANISM OF THREE STEP ATOMIC LAYER DEPOSITION (ALD) OF COPPER VIA FORMATE AND HYDRAZINE. THE TECHNIQUE HOLDS PROMISE FOR DEPOSITION OF OTHER TRANSITION METALS.

Introduction

Atomic Layer Deposition (ALD) is an innovative thin film deposition technique used today in the semiconductor industry. In principle it facilitates the deposition of materials atomic layer by atomic layer. Thus the thickness of the materials can be controlled at the sub nm level.

Copper is an important material in the semiconductor industry as it is used as the electrical interconnecting material within integrated circuits. For continued downscaling of electronic devices, a continuous Cu film < 2 nm thick is required as the seed layer for subsequent electrodeposition of copper interconnect. However, a problem arises as copper tends to agglomerate into discrete islands at typical deposition temperatures. This issue has received wide scale attention and is listed as one of the major problems in the semiconductor technology roadmap[1].

Many attempts have been made to solve this problem by changing the precursor combination for Cu ALD. There have been reports of using $Cu(hfac)_2$ and alcohol (hfac=1,1,1,5,5,5-hexafluoro-3,5-pentanedionate)[2] at 300°C, CuCl and hydrogen as the reducing agent[3] at > 360°C and $Cu(thd)_2$ and hydrogen (thd = 2,2,6,6-tetramethyl-3,5-heptanedionate)[4] at 260°C. An organometallic reagent can also be used as the reducing agent e.g. $Cu(dmap)_2$ and $ZnEt_2$ (dmap = $OCHMeCH_2$-NMe_2)[5] at 100°C. $Cu^{(+1)}$ compounds were also tested but the process appears to be closer to pulsed Chemical Vapour Deposition (CVD) rather than ALD[6]. Vidjayacoumar *et al.*[7,8] reported using BEt_3, $AlMe_3$ and $ZnEt_2$ in solution phase as prospective reducing agents and obtained a copper deposit from $ZnEt_2$ but not from BEt_3 and $AlMe_3$. A parasitic reaction was reported with $ZnEt_2$, which leads to Zn impurity. A mechanistic study using Density Functional Theory (DFT) has been reported by Dey and Elliott[9] on these transmetallation reactions.

All the techniques mentioned above have high reaction temperatures. Knisley *et al.*[10,11] proposed a new technique for Cu ALD at low temperature. They have reported that the deposition starts from 80°C and that the growth rate becomes constant at 120°C, with no growth seen above 160°C. Each ALD cycle consists of three pulses: $Cu(dmap)_2$, a protic acid (formic acid) and hydrazine. Knisley's proposal holds promise for deposition of other metals too, with initial results reported from $Ni^{(+2)}$ complexes[11].

The proposed overall growth reaction in each ALD cycle independent of the surface can be written as follows:

$$Cu(dmap)_{2(g)} + 2HCOOH_{(g)} + N_2H_{4(g)} \rightarrow Cu^{(0)}_{(s)} + 2CO_{2(g)} + 2dmap\text{-}H_{(g)} + 2NH_{3(g)} \quad \ldots.(1)$$

Knisley *et al.* propose that this reaction proceeds via a copper formate surface intermediate after the HCOOH pulse, but there is no direct evidence for this intermediate in their work. However, Ravindranathan *et al.*[12] have shown by chemical analysis and infrared spectroscopy that an aqueous solution of copper formate undergoes rapid reduction to copper metal at ambient temperature upon treatment with hydrazine hydrate. Hydrazine has been used previously as a catalytic reducing agent for aromatic nitro compounds in the presence of finely divided metals[13], but equation (1) implies that N is itself reduced along with Cu in this case. The mechanistic detail of this ALD process remains conjectural and this forms the motivation for our work.

Method

We apply Unrestricted DFT using the Perdew−Burke−Ernzerhof (PBE) functional[14] and the valence double-ζ with polarization def-SV(P) all-electron basis set[15], as implemented in the TURBOMOLE program version 6.4[16,17]. A Cu_{55} cluster 'coin' with a (111) surface facet of C_{3v} symmetry has been modelled so as to understand the adsorption of the compounds. All the adsorbed models were computed with zero total charge. The surface model has been used by Larsson *et al.*[18]. TURBOMOLE is limited to gas phase or cluster calculations. Therefore, in order to calculate total energies per Cu atom of bulk Cu metal for the reaction energies, we add the adhesion energy computed for bulk $Cu_{(s)}$ using the VASP code[19] with the same functional. Here valence electron states are expanded in a plane-wave basis set with an energy cutoff of 300 eV and with the projected augmented wave treatment of cores. The electron exchange and correlation were treated with the same PBE functional. For the bulk copper, k-point sampling is performed with an 8x8x8 Monkhorst-Pack sampling grid. The bulk lattice constant is determined using the Murnaghan equation of state. The adhesion energy has been added to the energy change for reaction steps that

feature metallic copper formation. The technique used here has also been reported in earlier studies[9,20]. Through various experimental and theoretical calculations comparing the properties of copper, it has been seen that relativistic effects are not relevant for Cu metal[21]. Hence, no relativistic effects have been taken into account.

The entropy change for the reactions has also been calculated. This is done by vibrational analysis of the gas phase molecules using TURBOMOLE[22]. The entropy has been calculated at T=393 K as this is a typical target temperature for Cu ALD. It is assumed that S(Molecule+Coin) ≈ S(Coin) + S_{vibr}(Molecule) and so the entropy change is $\Delta S_{ad} \approx -S_{trans+rot}$(Molecule). This is because, after the molecule is adsorbed onto the surface, it loses its translational and rotational degrees of freedom and this is probably the major contribution to the entropy change. *Ab initio* Molecular Dynamics (MD) within the isothermal-isobaric ensemble as implemented in TURBOMOLE has been carried out for a set of model structures for a duration of 2 ps.

Results and Discussion

In order to understand the mechanism we will pose a series of questions in the following sections. Reactions that are thermodynamically favoured have negative reaction energies. The set of reactions presented here are the most energetically feasible ones out of the wide range that we have investigated.

For each of the three steps in the ALD cycle, we seek to understand the reaction process at the surface:

a) Interaction of the precursor with the surface

Surface + $Cu^{(2+)}(dmap)_{2(g)} \rightarrow Cu^{(2+)}(dmap)_{2(ads)} \rightarrow Cu^{(+1)}(dmap)_{(ads)}$

b) Interaction of formic acid with the precursor fragments:

$Cu^{(+1)}(dmap)_{(ads)} + HCOOH_{(g)} \rightarrow ?$

c) Interaction of hydrazine with the precursor and formic acid fragments:

$Cu^{(+1)}(dmap)_{(ads)} + HCOOH_{(ads)} + NH_2\text{-}NH_{2(g)} \rightarrow ?$

Step (a) is described in previous studies[9] and we take the conclusion from the papers to build our starting model. Step (b) is investigated in section (i). Step (c) is investigated in sections (ii) and (iii).

(i) How do precursor fragments interact with formic acid?

When $Cu(dmap)_2$ adsorbs to a Cu surface, its most stable state is found[9,23] to be $Cu^{(+1)}(dmap)$. Therefore, in order to understand the further interaction with formic acid, we have taken a model system that has one dmap ligand adsorbed to a Cu (111) surface. This shows an adsorption energy of ΔE_{ad} = -647 kJ/mol relative to the gas-phase dmap anion and cationic coin (Table 1, Figure 1(i)).

To the optimised geometry of this $Cu^{(+1)}$dmap adsorbate we brought in HCOOH (Figure 2). During a 300 step MD study of 2 ps duration, at 393 K from this geometry, we see that the oxygen of the dmap anion on the surface spontaneously abstracts the protonic H from formic acid (floating near it) to form a protonated ligand dmap-H. The spontaneous abstraction of the proton within 2 ps indicates that the activation energy can be readily overcome at T = 393 K. The remaining formate anion ($HCOO^-$) bonds with a copper atom on the surface. The optimized structure of adsorbed HCOOH shows ΔE_{ad} = -33 kJ/mol onto the bare copper surface (Table 1, Figure 1 (ii)). The adsorption energy of the formate anion alone is ΔE_{ad} = -565 kJ/mol relative to the gas-phase anion (Table 1). The overall reactions with desorption of the dmap-H ligand and adsorption of formate anion may thus be written:

$dmap^-_{(surf)} + HCOOH_{(g)} \rightarrow dmap\text{-}H_{(g)} + HCOO^-_{(surf)}$ ….(2)

This reaction is computed to be exothermic: ΔE = -56 kJ/mol at T=0 K.

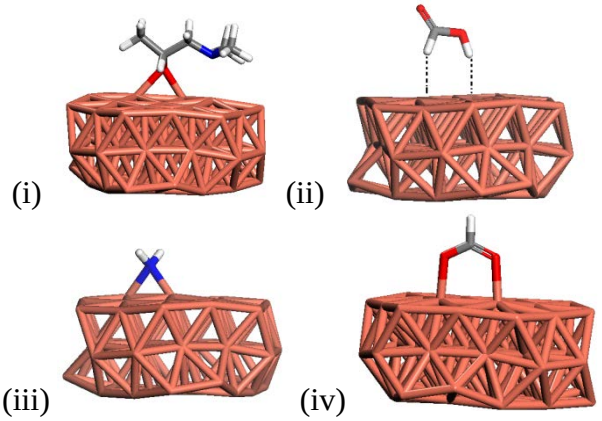

Figure 1: Optimized structure of (i) dmap ligand adsorbed on the smooth model copper surface, (ii) physisorbed formic acid, (iii) adsorbed NH_2 radical, (iv) adsorbed formate anion (Figure 3 for formate adsorption onto a rough surface). Colour code: brown=Cu, blue=N, red=O, grey=C, white=H.

Table 1: Adsorption energies (ΔE_{ad}), entropy contribution ($T\Delta S_{ad}$) of the molecules at T=393 K and free energies (ΔG_{ad}) of adsorption for anionic ligands and neutral molecules onto the copper surface, all relative to optimum gas-phase geometries. All the energies are in kJ/mol.

Adsorbate	ΔE_{ad}	$T\Delta S_{ad}$	ΔG_{ad}
$dmap^-$	-647.0	-182.0	-465.0
$HCOO^-$	-565.0	-93.4	-471.6
HCOOH	-33.0	-95.1	62.1
NH_2	-240.0	-56.8	-183.2
N_2H_4	-109.0	-140.0	31
NH_3	-42.0	-95.8	53.8
CO_2	23.0	-39.7	62.7

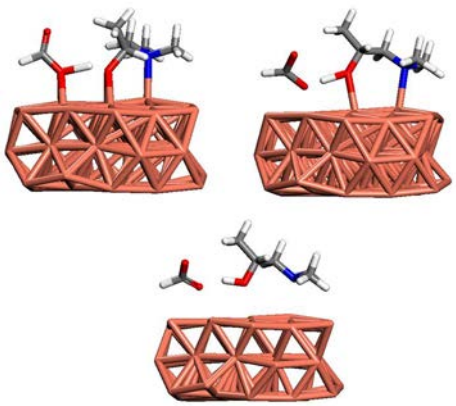

Figure 2: Some snapshots of MD simulation of dmap anion interacting with formic acid in order to form copper formate and dmap-H. The above structures are not optimized. Colour code: brown=Cu, blue=N, red=O, grey=C, white=H.

Table 2: Reaction energies ΔE, entropy change ($T\Delta S$) at T = 393 K and the free energy ΔG for the gas phase dissociation of the NH_2-NH_2 and $(CH_3)_2N$-NH_2 molecules. All the energies are in kJ/mol.

Reaction No.	Reaction	ΔE	$T\Delta S$	ΔG
4	NH_2-NH_2 → $2NH_2$	54.7	32.6	22.1
5	NH_2-NH_2 → NH + NH_3	44.9	24.0	20.9
6	NH_2-NH_2 → N_2 + $2H_2$	209.8	63.2	146.6
7	$(CH_3)_2N$-NH_2 → $(CH_3)_2N$ + NH_2	293.0	28.6	264.4
8	$(CH_3)_2N$-NH_2 → NH + $(CH_3)_2NH$	270.0	20.4	249.6
9	$(CH_3)_2N$-NH_2 → N_2 + $2CH_4$	400.0	36.0	364.0

(ii) How does the hydrazine react?

$Cu^{(+1)}OOCH_{(surf)} + ½.N_2H_{4(g)} \rightarrow Cu^{(0)}{}_{(s)} + CO_{2(g)} + NH_{3(g)}$

ΔE = -272 kJ/mol …. (3)

Knisley *et al.*[11] propose that hydrazine reacts with surface adsorbed copper formate to deposit copper and form gaseous by-products (eq. 3 above). We compute that the reaction is exothermic and therefore plausible.

We are interested in the possible pathway for this step. Hydrazine might disintegrate into active species when it comes in contact with the surface (surface catalysed reaction[12]) or else thermal energy might split the molecule in the gas phase already. In order to find out what active species are likely to be present when hydrazine is admitted to the chamber, we have computed the possible dissociation reactions of hydrazine in the gas phase, as given in Table 2 (reaction no. 4-6). The $T\Delta S$ contribution at T =393 K is 32.6 kJ/mol, 24.0 kJ/mol and 63.2 kJ/mol for equations 4, 5 and 6 respectively. Thus the entropy contribution makes the total ΔG ~ 20 kJ/mol for equations (4) and (5), which suggests that the formation of gas phase radicals NH_2 or NH is possible with some additional thermal energy. However, ΔG is > 140 kJ/mol for equation (6), so that N_2 and H_2 are unlikely to be formed. The use of NH_2 radicals in the formation of pure metals like Co has been investigated before by Hideharu *et al.*[24]

We compute the energy of adsorption (Table 1) of a NH_2 radical onto the Cu surface to be ΔE_{ad} = -240 kJ/mol-NH_2 (Figure 1 (iii)). Molecular adsorption of N_2H_4 shows ΔE_{ad} = -109 kJ/mol (Table 1). Hence, by Hess's law we see that surface formation of $NH_{2(ads)}$ from $N_2H_{4(ads)}$ releases -317 kJ/mol of energy (Figure 3). These high adsorption energies might indicate that N persists at the surface as an impurity in the film. However, we know that Cu_3N is an unstable compound[25] and so ultimately N incorporation is probably not favoured. The formation of NH from N_2H_4 is not explored as it is unreactive over a surface, which will be seen in the next section.

Thus the disintegration of hydrazine takes place either in the gas phase into NH_2 and NH or over the surface into NH_2. The computed energetics favour the latter, but the process that actually predominates will depend on the relative kinetics under specific reactor conditions.

The gas phase dissociation of 1,1-dimethyl hydrazine can be compared with that of NH_2-NH_2. The reaction energies (ΔE) are given in Table 2 (reaction no. 7-9). The $T\Delta S$ for reaction (7) is 28.6 kJ/mol, for (8) is 20.4 kJ/mol and for (9) is 36.0 kJ/mol. Thus the entropy factor cannot overcome the unfavourable reaction energies. This suggests that hydrazine is a better source of NH_x radicals (x=1, 2) than substituted hydrazine.

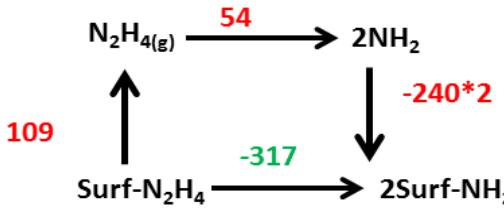

Figure 3: Hess cycle showing the formation of surface adsorbed NH_2 from surface adsorbed N_2H_4. All the energies are in kJ/mol of hydrazine.

(iii) How do the NH_x radicals react with copper formate?

To investigate the subsequent reactions, we have brought the NH and NH_2 radicals close to the atoms of the adsorbed copper formate moiety from the previous reaction steps and optimized the geometry. The possible sites for NH and NH_2 attack are Cu, O and H.

We see that when we bring the NH_2 towards Cu, perpendicular to the plane of the adsorbed copper formate, it forms a Cu-N adduct, without any further change. When the radical is brought towards formate H or towards O in same plane as the formate moiety (Figure 4), it abstracts the H and spontaneously forms NH_3 and CO_2 during the geometry optimization. The spontaneous formation of Cu and the by-products at T = 0 K indicate that there is no activation energy at this temperature.

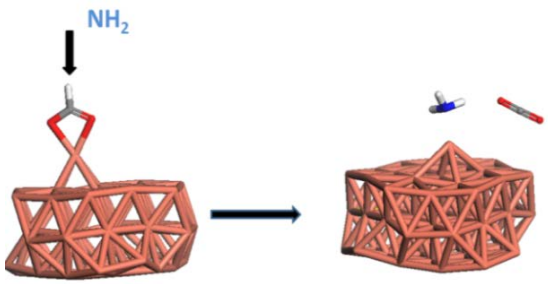

Figure 4: When the NH_2 radical attacks the H of Cu(HCOO), it forms CO_2 and NH_3 as by-products, leaving an atom of copper metal on the surface. Colour code: brown=Cu, blue=N, red=O, grey=C, white=H.

For the gas-surface reaction that we have observed we compute the following energy change:

$Cu^{(+1)}OOCH_{(surf)} + NH_{2(g)} \rightarrow Cu^{(0)}{}_{(s)} + CO_{2(g)} + NH_{3(g)}$

ΔE = -467 kJ/mol …. (10)

However, as shown in section (ii) above, NH_2 most likely originates at the surface and so, by subtracting ΔE_{ad} = -240 kJ/mol (Table 1) from ΔE for equation (10), we can write the following surface reaction:

$Cu^{(+1)}OOCH_{(surf)} + NH_{2(surf)} \rightarrow Cu^{(0)}{}_{(s)} + CO_{2(g)} + NH_{3(g)}$

ΔE = -227 kJ/mol …. (11)

The $T\Delta S$ for reaction (11) is 78.7 kJ/mol at T = 393 K and thus ΔG is -305.7 kJ/mol. Redistribution of the reaction energy from equation (11) would thus be sufficient to break even the N-N bond in hydrazine (~50 kJ/mol, equation 3) and desorb the by-products from the surface.

Here we see that the C in $Cu^{(+1)}OOCH$ is in its +2 oxidation state and transforms to +4 oxidation state in CO_2 giving away one electron to $N^{(-2)}H_2$ to form $N^{(-3)}H_3$ and another electron to $Cu^{(+1)}$ to form $Cu^{(0)}$.

Following a similar approach, the NH radical was placed in a plane perpendicular to the copper formate at different positions, close to Cu, H and O. In all the cases we find that the NH moves close to the surface atoms and away from the adsorbed copper formate during optimization. The NH then attaches itself to the coordinatively unsaturated Cu atoms on the surface.

Finally, we compute the adsorption energy of the by-products: $\Delta E_{ad}(NH_3)$ = -42.0 kJ/mol and $\Delta E_{ad}(CO_2)$ = +23.0 kJ/mol at T=0 K (Table 1). At T=393 K the $T\Delta S$ is 95.8 kJ/mol for NH_3 (Ref.[20]) and for CO_2 is 39.7 kJ/mol. Hence the adsorption of these by-products is thermodynamically not favoured

We calculate that ΔE_{ALD}= -172 kJ/mol-Cu at T=0 K (Table 4) for the three-step growth process described in equation (1), by making use of the adhesion energy of bulk Cu of -320 kJ/mol-Cu calculated with VASP[9]. The overall ALD cycle is therefore exothermic.

To summarise, we have observed in the above reactions that NH_2 radicals are formed after the surface-mediated dissociation of the hydrazine molecule and that they react spontaneously with adsorbed copper formate to deposit copper and produce CO_2 and NH_3 by-products. Each of the mechanistic steps is exothermic and some are barrierless. The overall cycle is also exothermic. This provides evidence that equation (1) takes place as proposed by Knisley *et al.*

Table 3: Computed reaction energies (ΔE) of key steps in the 3-step ALD process.

Reaction No.	Reaction	ΔE (kJ/mol)
2	$dmap^-_{(surf)} + HCOOH_{(g)} \rightarrow dmap\text{-}H_{(g)} + HCOO^-_{(surf)}$	-56
11	$Cu^{(+1)}OOCH_{(surf)} + NH_{2(ad)} \rightarrow Cu^{(0)}_{(s)} + CO_{2(g)} + NH_{3(g)}$	-227

(iv) How does hydrazine react with higher acid copper compounds?

Now that we have some insights into the mechanism, it is interesting to ask whether other protonic acids can function in the same way as formic acid in this process. The above reaction process (1) was altered so as to consider acetic acid in equation (12) and propanoic acid in equation (13), listed in Table 4.

Table 4: Energies for the total ALD growth process (ΔE_{ALD}) using hydrazine, organic acids and dmap precursor.

Reaction No.	Reaction	ΔE_{ALD} (kJ/mol)
1	$Cu(dmap)_{2(g)} + 2HCOOH_{(g)} + N_2H_{4(g)} \rightarrow Cu^{(0)}_{(s)} + 2CO_{2(g)} + 2dmap\text{-}H_{(g)} + 2NH_{3(g)}$	-172
12	$Cu(dmap)_{2(g)} + 2CH_3COOH_{(g)} + NH_2\text{-}NH_{2(g)} \rightarrow Cu^{(0)}_{(s)} + 2dmap\text{-}H_{(g)} + 2CO_{2(g)} + 2CH_3\text{-}NH_{2(g)}$	-58
13	$Cu(dmap)_{2(g)} + 2CH_3CH_2COOH_{(g)} + NH_2\text{-}NH_{2(g)} \rightarrow Cu^{(0)}_{(s)} + 2dmap\text{-}H_{(g)} + 2CO_{2(g)} + 2CH_3CH_2\text{-}NH_{2(g)}$	-98
14	$Cu(dmap)_{2(g)} + 2CH_3COOH_{(g)} + NH_2\text{-}NH_{2(g)} \rightarrow Cu^{(0)}_{(s)} + 2dmap\text{-}H_{(g)} + 2CO_{2(g)} + 2NH_{3(g)} + CH_2{=}CH_{2(g)}$	+18
15	$Cu(dmap)_{2(g)} + 2CH_3CH_2COOH_{(g)} + NH_2\text{-}NH_{2(g)} \rightarrow Cu^{(0)}_{(s)} + 2dmap\text{-}H_{(g)} + 2CO_{2(g)} + 2NH_{3(g)} + 2CH_2{=}CH_{2(g)}$	+90

This assumes that the NH_2 radical abstracts an alkyl radical from adsorbed acetate or propanoate, breaking a C-C bond. The computations yielded ΔE_{ALD}= -58 kJ/mol for equation (12) and -98 kJ/mol for equation (13). The exothermicity indicates that these processes may take place. These ALD energies are less negative than that of equation (1), which may be attributed to the cost of breaking the strong C-C bond in these acids.

To investigate this reaction pathway, we bring the NH_2 radical near to the structure of adsorbed copper acetate, and observe during geometry optimization that the NH_2 radical coordinates with the coordinatively unsaturated surface copper atoms, rather than spontaneously abstracting the methyl radical. This indicates high activation energy. Thus, although the overall ALD reaction energy is moderately exothermic, energy barriers exist that make the surface-mediated reaction with higher acids less likely to take place than in the previous case of HCOOH. Nevertheless, the reaction might proceed via this mechanism depending on temperature and external conditions, *e.g.* in the solution phase, as mentioned by Knisley *et al.*[11].

Alternative by-products for the higher acids are suggested in reaction no. 14-15 (Table 4), via reductive elimination of H from the alkyl groups (*i.e.* breaking C-H rather than C-C). We compute ΔE_{ALD}=+18 kJ/mol overall for (14) and +90 kJ/mol for (15) indicating that these ALD cycle are endothermic and less probable than processes (12) and (13).

Conclusions

DFT calculations have been used to investigate the surface reactions of a three step ALD process for the deposition of Cu as proposed by Knisley *et al.*[11] Those authors proposed the formation of intermediate Cu formate at the surface and its reaction with hydrazine. Here, we confirm the stability of the formate intermediate and find the atom-by-atom mechanism for the reaction with hydrazine and deposition of Cu metal. All the elementary reaction steps are computed to be exothermic and many of the reaction steps are barrierless.

It has previously been computed that the $Cu(dmap)_2$ precursor adsorbs strongly to the surface, which is the first step of the ALD cycle. In the second step formic acid is pulsed into the chamber. It is observed in our simulation that the dmap ligand abstracts the protonic H from formic acid and desorbs as dmap-H, leaving formate adsorbed to the surface. In the final step, hydrazine is pulsed into the chamber and probably dissociates at the surface to form the NH_2 radical. This radical abstracts $H^{(0)}$ from the formate anion. Spontaneous decomposition of the resulting anion to CO_2 causes reduction of a surface metal cation to $Cu^{(0)}$. The predicted by-products during this step are NH_3 and CO_2.

We find therefore that hydrazine partially *oxidises* formate, which through its complete decomposition to CO_2 *reduces* $Cu^{(+1)}$ to $Cu^{(0)}$ (Figure 5). This suggests that the search for co-reagents in metal ALD should not be limited to traditional reducing agents like H_2, but can also include reagent combinations that release electrons during oxidative decomposition.

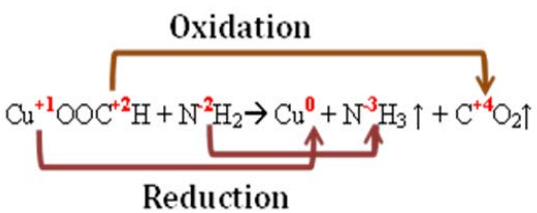

Figure 5: Redox reaction of equation 1

Acknowledgements

We are grateful to Science Foundation Ireland for funding under the ALDesign project, grant number 09.IN1.I2628, http://www.tyndall.ie/aldesign and to Prof. C. H. Winter of Wayne State University for useful discussion.

[a]*Tyndall National Institute University College Cork, Lee Maltings, Cork, Ireland. Tel: +353 21 234 6392; E-mail: gangotri.dey@tyndall.ie*

[b]*Tyndall National Institute, University College Cork, Lee Maltings, Cork, Ireland. Fax: +353 21 490 4058; Tel: +353 21 234 6392; E-mail: simon.elliott@tyndall.ie*

Reference:

(1) International Technology Roadmap for Semiconductors *http://www.itrs.net/*, 2011
(2) Solanki, R.; Pathangey, B. Electrochemical and Solid-State Letters **2000**, 3, 479.
(3) Mårtensson, P.; Larsson, K.; Carlsson, J.-O. Applied Surface Science **2000**, 157, 92.
(4) Hsu, I. J.; McCandless, B. E.; Weiland, C.; Willis, B. G. Journal of Vacuum Science & Technology A: Vacuum, Surfaces, and Films **2009**, 27, 660.
(5) Lee, Soo G.; Kim, Yun J.; Lee, Seung P.; Oh, H.-S.; Lee, Seung J.; Kim, M.; Kim, I.-G.; Kim, J.-H.; Shin, H.-J.; Hong, J.-G.; Lee, H.-D.; Kang, H.-K. Japanese Journal of Applied Physics **2001**, 40, 2663.
(6) Thompson, J. S.; Zhang, L.; Wyre, J. P.; Brill, D. J.; Lloyd, K. G. Thin Solid Films **2009**, 517, 2845.
(7) Vidjayacoumar, B.; Emslie, D. J. H.; Clendenning, S. B.; Blackwell, J. M.; Britten, J. F.; Rheingold, A. Chemistry of Materials **2010**, 22, 4844.
(8) Vidjayacoumar, B.; Emslie, D. J. H.; Blackwell, J. M.; Clendenning, S. B.; Britten, J. F. Chemistry of Materials **2010**, 22, 4854.
(9) Dey, G.; Elliott, S. D. The Journal of Physical Chemistry A **2012**, 116, 8893.
(10) Knisley, T. J.; Kalutarage, L. C.; Winter, C. H. Coordination Chemistry Reviews **2013**, 257, 3222.
(11) Knisley, T. J.; Ariyasena, T. C.; Sajavaara, T.; Saly, M. J.; Winter, C. H. Chemistry of Materials **2011**, 23, 4417.
(12) Ravindranathan, P.; Patil, K. C. Thermochimica Acta **1983**, 71, 53.
(13) Furst, A.; Berlo, R. C.; Hooton, S. Chemical Reviews **1965**, 65, 51.
(14) Perdew, J. P.; Burke, K.; Ernzerhof, M. Physical Review Letters **1996**, 77, 3865.
(15) Schafer, A.; Horn, H.; Ahlrichs, R. The Journal of Chemical Physics **1992**, 97, 2571.
(16) Ahlrichs, R.; Bär, M.; Häser, M.; Horn, H.; Kölmel, C. Chemical Physics Letters **1989**, 162, 165.
(17) Schafer, A.; Huber, C.; Ahlrichs, R. The Journal of Chemical Physics **1994**, 100, 5829.
(18) Larsson, J. A.; Elliott, S. D.; Greer, J. C.; Repp, J.; Meyer, G.; Allenspach, R. Physical Review B **2008**, 77, 115434.
(19) Kresse, G.; Hafner, J. Physical Review B **1994**, 49, 14251.
(20) Dey, G.; Elliott, S. Theor Chem Acc **2013**, 133, 1.
(21) Iliaš, M.; Kellö, V.; Urban, M.; Urban, M. Acta Physica Slovaca. Reviews and Tutorials 2010, 60, 259
(22) Deglmann, P.; May, K.; Furche, F.; Ahlrichs, R. Chemical Physics Letters **2004**, 384, 103.
(23) Coyle, J. P.; Dey, G.; Sirianni, E. R.; Kemell, M. L.; Yap, G. P. A.; Ritala, M.; Leskelä, M.; Elliott, S. D.; Barry, S. T. Chemistry of Materials **2013**, 25, 1132.
(24) Shimizu, H.; Sakoda, K.; Momose, T.; Koshi, M.; Shimogaki, Y. Journal of Vacuum Science & Technology A **2012**, 30.
(25) Gonzalez-Arrabal, R.; Gordillo, N.; Martin-Gonzalez, M. S.; Ruiz-Bustos, R.; Agullo-Lopez, F. Journal of Applied Physics **2010**, 107, 103513.